Membrane identity and GTPase cascades regulated by toggle and cut-out switches. Supplementary information

P. Del Conte-Zerial [1,2], L. Brusch[1], J. C. Rink[2], C. Collinet[2], Y. Kalaidzidis[2], M. Zerial[2] and A. Deutsch[1]

1. *Center for Information Services and High Performance Computing, University of Technology Dresden, 01062 Dresden, Germany*

2. *Max Planck Institute of Molecular Cell Biology and Genetics, Pfotenhauer Straße 108, 01308 Dresden, Germany*

Contents

List of Figures

List of Tables

1 Model Definition: Differential Equations System, GEF and GAP kinetics

The mathematical model consists of four ordinary differential equations based on the biochemical protein-protein interactions of Rab5 and Rab7. The concentrations of Rab5:GDP, Rab5:GTP, Rab7:GDP and Rab7:GTP on the endosomal menrane are denoted as $r_5(t)$, $R_5(t)$, $r_7(t)$, $R_7(t)$, respectively. Their physical unit is *particle number per surface area*.

The concentrations may change according to the processes considered in Fig. 1 yielding the following equation system.

$$\begin{aligned}
\tfrac{dr_5}{dt} &= K_{-1} - (k_1 + GEF_5(R_5,R_7))r_5(t) + GAP_5(R_5,R_7)R_5(t) \\
\tfrac{dR_5}{dt} &= GEF_5(R_5,R_7)r_5(t) - GAP_5(R_5,R_7)R_5(t) \\
\tfrac{dr_7}{dt} &= K_{-2} - (k_2 + GEF_7(R_5,R_7))r_7(t) + GAP_7(R_5,R_7)R_7(t) \\
\tfrac{dR_7}{dt} &= GEF_7(R_5,R_7)r_7(t) - GAP_7(R_5,R_7)R_7(t)
\end{aligned} \tag{1}$$

$GEF_i(R_5,R_7)$ and $GAP_i(R_5,R_7)$, $i = 5,7$ are functions of the concentrations of the active forms of Rab5 and Rab7 denoting the reaction mechanism of GDP-GTP exchange and hydrolysis, respectively. Rab proteins only transiently interact with membranes and continuously shuttle between membrane association and cytosolic GDI-association. K_{-1} and K_{-2} denote the dissociation flux from GDI and k_1, k_2 the association rates with GDI. Concentrations of Rab-GDI and free GDI are considered to be constant and included in the parameter values. This coupling to the constant Rab-GDI pool renders the system open as opposed to other biomolecular switches that rely on the conservation of system components [1].

To analyze how different kinetics influence the steady states behavior of membrane associated Rab5:GTP and Rab7:GTP we screened different combinations of GEF and GAP kinetics as shown in **Table 1**. Parameter values were sampled from reasonable ranges. The phenomenon of bistability occurs in parameter intervals in which two stable states coexist which are separated by an unstable state. Leaving the bistability interval upon a parameter change the system relaxes towards the remaining stable state. Switching is not readily reversible by removing the stimulus, i.e. there is hysteresis and reversal generally requires a stronger, opposite stimulus.

2 Model screening: phase plane analysis

We set out to classify, by means of steady state properties, the large set of models that can be constructed by inserting combinations of rate laws for the experimentally unknown $GEF_5(R_5,R_7)$, $GAP_5(R_5,R_7)$, $GEF_7(R_5,R_7)$, $GAP_7(R_5,R_7)$. The problem of screening sets of models for corresponding biological behaviour and reproduction of experimental results has also been faced by other systems including oscillations of the somitogenesis clock [2]. Direct numerical simulation is the common approach to analyse systems with many variables. For a finite set of parameter samples, however, this approach doesn't guarantee to reveal the complete spectrum of model features. Limited computational resources restrict the size of the set of samples.

Here we benefit from the low dimensionality of the system with only four variables. We apply the analytical and graphical methods of phase plane analysis which request minimal computational effort and allow to conclude (for the entire high-dimensional parameter space) about the system behavior in terms of steady states, multistability and occuring bifurcations.

In order to test for steady states, we set the left hand sides of equation (1) to zero and insert the solutions of two equations $r_5 = \frac{K_{-1}}{k_1}$ and $r_7 = \frac{K_{-2}}{k_2}$ into the remaining equations

$$0 = \tfrac{dR_5}{dt} = GEF_5(R_5,R_7)\tfrac{K_{-1}}{k_1} - GAP_5(R_5,R_7)R_5,$$

$$0 = \tfrac{dR_7}{dt} = GEF_7(R_5,R_7)\tfrac{K_{-2}}{k_2} - GAP_7(R_7,R_5)R_7.$$

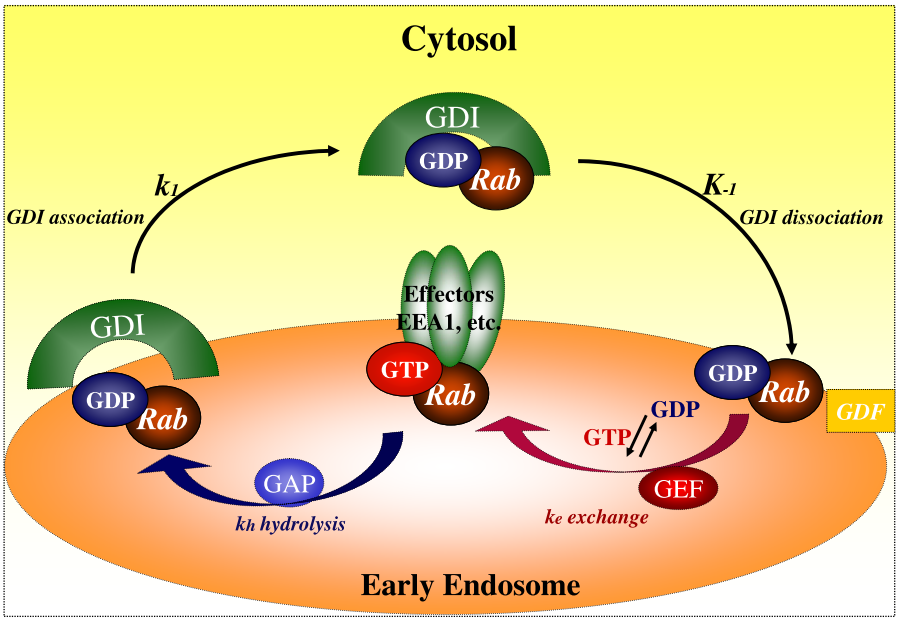

Figure 1: Rab proteins switch between the GTP-bound and GDP-bound conformation, defined here as the ON and OFF state, respectively. Rab GTPases are present in the cytosol in the OFF state bound to Rab-GDI, which delivers them to, and solubilises them from, the endosome membrane. After dissociation from Rab-GDI, catalyzed by GDI-Displacement factor (GDF), Rab proteins undergo continuous cycles of nucleotide exchange and hydrolysis. GDP/GTP nucleotide exchange is catalyzed by GEFs and hydrolysis of GTP to GDP by GAPs. In the GTP-bound form, Rab proteins interact with a set of effector proteins (e.g. EEA1, Rabaptin-5 for Rab5) that stabilize the ON state and execute functions in membrane transport, conferring structural and functional identity to the compartment harbouring them.

Rab5	**Type of kinetics**	**Non-linear rate law**
$GEF_5(R_5, R_7)$	Michaelis Menten kinetics	$\frac{k_{e,5} \cdot R_5}{k_{g,5}+R_5}$
$GEF_5(R_5, R_7)$	Sigmoidal response to Rab5	$\frac{k_{e,5}}{1+e^{(k_{g,5}-R_5)k_{f,5}}}$
$GEF_5(R_5, R_7)$	Exchange inhibition via Rab7 (Monod competitive inhibition)	$\frac{k_{e,5} \cdot R_5}{k_m(1+R_7/k_i)+R_5}$
$GAP_5(R_5, R_7)$	Sigmoidal response to Rab7	$\frac{k_{h,5}}{1+e^{(k_{H,5}-R_7)k_{y,5}}}$
$GAP_5(R_5, R_7)$	Michaelis Menten kinetics	$k_{h,5} + \frac{k_{H,5} \cdot R_7}{k_{y,5}+R_7}$
$GAP_5(R_5, R_7)$	Intrinsic hydrolysis	$k_{h,5}$
Rab7	**Type of kinetics**	**Non-linear rate law**
$GEF_7(R_5, R_7)$	Michaelis Menten activation	$\frac{k_{e,7} \cdot R_7}{k_{g,7}+R_7} + \frac{k_{E,7} \cdot R_5}{k_{G,7}+R_5}$
$GEF_7(R_5, R_7)$	Michaelis Menten auto-activation, Sigmoidal response to Rab7	$\frac{k_{e,7} \cdot R_7}{k_{g,7}+R_7} + \frac{k_{E,7}}{1+e^{(k_{G,7}-R_5)k_{F,7}}}$
$GEF_7(R_5, R_7)$	Sigmoidal response to Rab7, Michaelis Menten activation via Rab5	$\frac{k_{e,7}}{1+e^{(k_{g,7}-R_7)k_{f,7}}} + \frac{k_{E,7} \cdot R_5}{k_{G,7}+R_5}$
$GEF_7(R_5, R_7)$	Sigmoidal responses to Rab7 and Rab5	$\frac{k_{e,7}}{1+e^{(k_{g,7}-R_7)k_{f,7}}} + \frac{k_{E,7}}{1+e^{(k_{G,7}-R_5)k_{F,7}}}$
$GEF_7(R_5, R_7)$	Sigmoidal responses to Rab7, no activation via Rab5	$\frac{k_{e,7}}{1+e^{(k_{g,7}-R_7)k_{f,7}}}$
$GEF_7(R_5, R_7)$	No activation via Rab7, M. Menten activation via Rab5	$k_{e,7} + \frac{k_{E,7} \cdot R_5}{k_{G,7}+R_5}$
$GEF_7(R_5, R_7)$	No activation via Rab7, sigmoidal responses to Rab5	$k_{e,7} + \frac{k_{E,7}}{1+e^{(k_{G,7}-R_5)k_{F,7}}}$
$GAP_7(R_5, R_7)$	Intrinsic hydrolysis	$k_{h,7}$
$GAP_7(R_5, R_7)$	Michaelis Menten kinetics and intrinsic hydrolysis	$k_{h,7} + \frac{k_{H,7} \cdot R_5}{k_{y,7}+R_5}$

Table 1: Kinetic rate laws have been combinatorially inserted into equation (1).

The two equations can be rewritten in the form

$$\begin{aligned} R_7(R_5) &= f_1(R_5, k_1, ...k_i), \\ R_7(R_5) &= f_2(R_5, k_2, ...k_i), \end{aligned} \tag{2}$$

which constitute the two nullclines for $dR_5/dt = 0$ and separately $dR_7/dt = 0$ in the phase plane spanned by R_5 and R_7. The steady states of the original coupled system are given by the intersections of both nullclines. For each given set of parameter values $k_1, ...k_i$, the nullclines also correspond to steady state stimulus-response curves of two isolated subsystems, e.g. for $dR_5/dt = 0$ the steady state relation between the input (stimulus) R_5 and the output (response) R_7 is given by $R_7 = f_1(R_5, k_1, ...k_i)$.

We analytically calculated the nullclines to dR_5/dt and dR_7/dt for all GEF and GAP kinetics listed in **table 1**. **Figure 1** and **figure 2** show the typical shape of the nullclines $f_1(R_5, k_1, ...k_i)$ and $f_2(R_5, k_2, ...k_i)$ in the (R_5, R_7) phase plane. Note, the specific magnitude and scale of each nullcline depends on parameter values whereas the qualitative shape is (for the relevant region of the parameter space) independent of parameters.

The steady states of the coupled system are recovered by intersecting pairs of nullclines. We have classified the models by the number of intersections of the two nullclines $f_1(R_5, k_1, ...k_i)$, $f_2(R_5, k_2, ...k_i)$ which yields the number of coexisting steady states, see **table 2**. The model doesn't show any switching behaviour if only a single intersection of nullclines exists. If two intersections are found then only one state can be stable and the system may undergo a transcritical bifurcation that exchanges stability between the two steady states. In case of three or more intersections, bistability is possible. Hence this latter scenario identifies model candidates with a Rab7-Rab7 switch.

We further analysed the relative location of the detected intersections in the phase plane which allows to distinguish between dominance of Rab5:GTP or Rab7:GTP at steady state, see **figure 3**. If three intersections roughly line up on the diagonal then one state has both concentrations low whereas another has both high. We term this behaviour an in-phase switch which is known from toggle switches with mutual activation [4]. If, on the other hand, one intersection possesses high R_5 and low R_7 and another intersection the reverse then a model with the biologically relevant behaviour has been identified. For systems with an additional conservation relation, the latter behaviour is known from toggle switches with mutual inhibition [1].

3 Verification of the phase plane analysis: bifurcation analysis and simulations

The phase plane analysis has provided the understanding of how bistability can be achieved for many model variants. Next we have to verify that upon parameter the existence of bistability in the selected models can variation be exploited as a switch between the coexisting stable states. The bifurcation analysis allows to determine the possible stable/unstable states of Rab5:GTP and Rab7:GTP as functions $\overline{R}_5(k_i)$, $\overline{R}_7(k_i)$ of a control parameter (k_i). We employed the method of numerical continuation to compute steady state solutions along branches for selected control parameters.

We used the software package AUTO [3]. Therein the solutions are represented as the root of an extended system of algebraic equations derived by discretizing the ODEs. Any new solution (the root) is then computed iteratively by the Newton algorithm. The software also monitors the linear stability of the solutions and thereby detects critical values of the parameters where the solutions change drastically, so called *bifurcations*. The critical parameter values where stable solutions cease existence are of special interest. One universal scenario for such vanishing of a stable solution occurs in phase plane terms via the coalescence and annihilation of the stable solution (called a node) with an unstable solution (called a saddle). The bifurcation occuring at the critical parameter value is then called a saddle-node bifurcation. Pairs of such saddle-node bifurcations

GEF_5 (R_5 R_7)	M.Menten kinetics		Sigmoidal response to R_5			Inhibition via Rab_7	Rab_7 activation via Rab_5	Rab_7 auto-activation	GAP_7 (R_5,R_7)
GAP_5 (R_5 R_7)	$k_{h,5}$ + M.Menten kinetics	Sigmoidal response to Rab_7	$k_{h,5}$ + M.Menten kinetics	Sigmoidal response to Rab_7	$k_{h,5}$	$k_{h,5}$			
A							M.Menten kinetics	M.Menten kinetics	Intrinsic hydrolysis $k_{h,7}$
B							Sigmoidal response to Rab_5		
C							M.Menten kinetics	Sigmoidal response to Rab_7	
D							Sigmoidal response to Rab_5		
E							No activation via Rab_5		
F							M.Menten kinetics	$k_{c,7}$	
G							Sigmoidal response to Rab_5		
H							Sigmoidal response to Rab_5	M.Menten kinetics	$k_{h,7}$+M.Menten kinetics
I							M.Menten kinetics		
	1	2	3	4	5	6			

Table 2: **54 model variants resulting from combinations of different GEF- and GAP-kinetics for Rab5 and Rab7.** Columns correspond to possible choices for Rab5-related reactions, rows to Rab7. Trivial models with monostability have been omitted in this table. Green areas denote models that can reproduce the switching from Rab5- to Rab7-dominated steady states. One portion of these constitutes a toggle switch, the other a cut-out switch. Yellow marks in-phase switches and red flaggs models without any bistability. Note that the cooperativity of at least one of the auto-activating GEF reactions is a necessary condition for the system to show bistability.

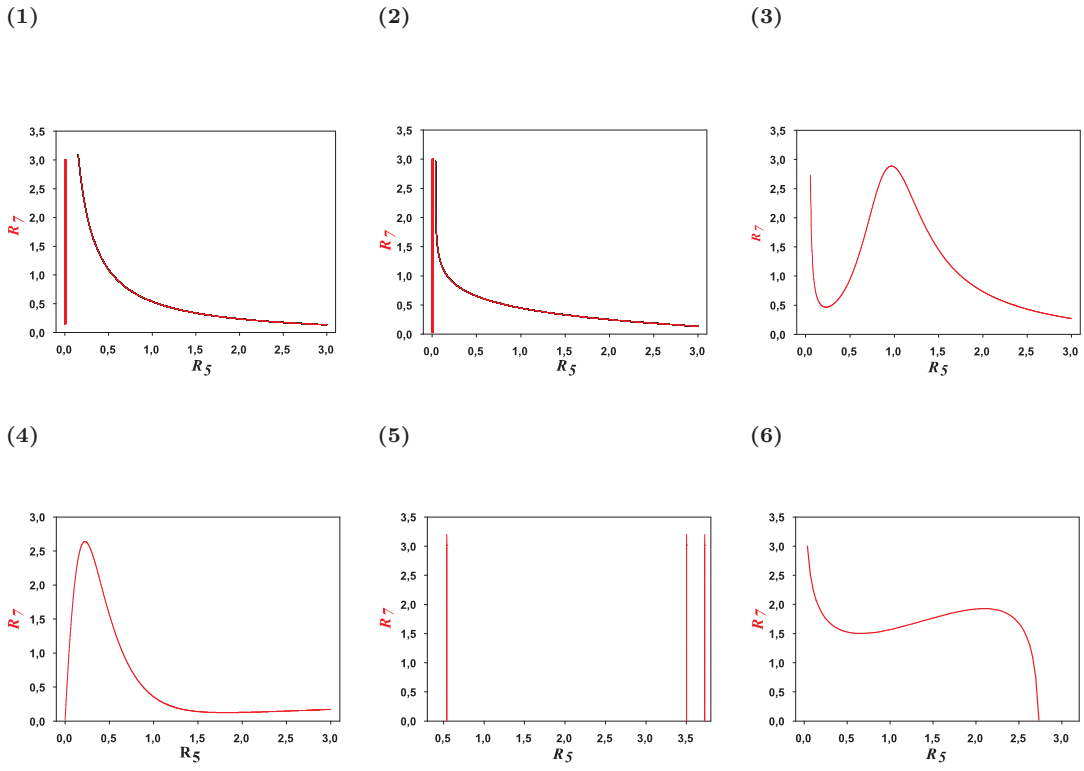

Figure 2: **Phase plane analysis of nullclines to dR_5/dt.** The 6 panels correspond to the 6 columns of **table 2**. Parameter values were chosen such that the essential features of all nullclines are scaled to the same axis range. **(1)** nullcline for column **1**, table 2, parameter values: $K_{-1}/k_1 = 1.00\ Units$; $k_{e,5} = 0.554\ s^{-1}$; $k_{g,5} = 1.20\ Units$; $k_{H,5} = 0.42\ s^{-1}$; $k_{h,5} = 0.06\ s^{-1}$; $k_{y,5} = 0.65\ Units$. **(2)** nullcline for column **2**, table 2, parameter values: $K_{-1}/k_1 = 1.00\ Units$; $k_{e,5} = 0.17\ s^{-1}$; $k_{g,5} = 0.15\ Units$; $k_{h,5} = 0.90\ s^{-1}$; $k_{y,5} = 3.60\ Units$. **(3)** nullcline for column **3**, table 2, parameter values: $K_{-1}/k_1 = 1.00\ Units$; $k_{e,5} = 0.053\ Units \cdot s^{-1}$; $k_{g,5} = 0.70\ Units$; $k_{f,5} = 4.80\ Units$; $k_{h,5} = 0.01\ s^{-1}$; $k_{H,5} = 0.05\ s^{-1}$; $k_{y,5} = 1.50\ Units$. **(4)** nullcline for column **4**, table 2, parameter values: $K_{-1}/k_1 = 1.00\ Units$; $k_{e,5} = 0.70\ Units \cdot s^{-1}$; $k_{g,5} = 1.30\ Units$; $k_{f,5} = 4.50\ Units$; $k_{H,5} = 0.004\ s^{-1}$; $k_{h,5} = 0.01\ Units$; $k_{y,5} = 0.20\ Units$. **(5)** nullcline for column **5**, table 2, parameter values: $K_{-1}/k_1 = 1.00\ Units$; $k_{e,5} = 0.26\ Units \cdot s^{-1}$; $k_{f,5} = 3.50\ Units$; $k_{g,5} = 1.40\ Units$; $k_{h,5} = 1.30\ Units$. **(6)** nullcline for column **6**, table 2, parameter values: $K_{-1}/k_1 = 1.00\ Units$; $k_{e,5} = 0.055\ s^{-1}$; $k_{i,5} = 0.40\ Units$; $k_{m,5} = 0.26\ Units$; $k_{h,5} = 0.02\ s^{-1}$. *Units* stands for *particle number per surface area.*

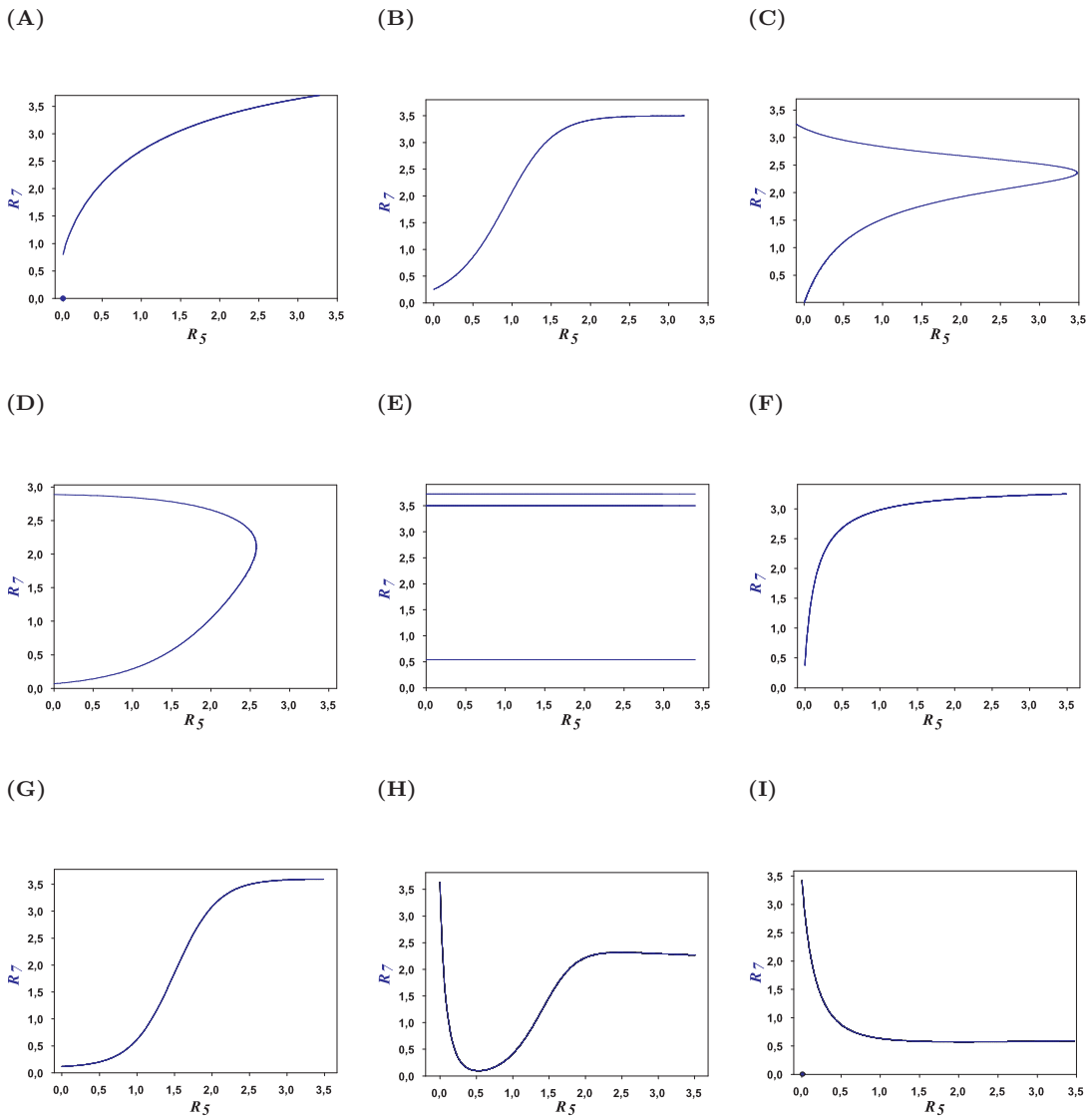

Figure 3: **Phase plane analysis of nullclines to** dR_7/dt**.** The 9 panels correspond to the 9 rows of **table 2**. Parameter values were chosen such that the essential features of all nullclines are scaled to the same axis range. **(A)** nullcline for row **A**, table 2, parameter values: $K_{-2}/k_2 = 1.00\ Units$; $k_{e,7} = 0.50\ s^{-1}$; $k_{g,7} = 1.70\ Units$; $k_{E,7} = 0.58\ s^{-1}$; $k_{G,7} = 1.50\ Units$; $k_{h,7} = 0.20\ s^{-1}$. **(B)** nullcline for row **B**, table 2, parameter values: $K_{-2}/k_2 = 1.00\ Units$; $k_{e,7} = 0.60\ s^{-1}$; $k_{g,7} = 2.50\ Units$; $k_{E,7} = 0.70\ Units \cdot s^{-1}$; $k_{G,7} = 1.00\ Units$; $k_{F,7} = 4.50\ Units$; $k_{h,7} = 0.30\ s^{-1}$. **(C)** nullcline for row **C**, table 2, parameter values: $K_{-2}/k_2 = 1.00\ Units$; $k_{e,7} = 0.50\ Units \cdot s^{-1}$; $k_{g,7} = 3.40\ Units$; $k_{f,7} = 3.30\ Units$; $k_{E,7} = 0.12\ s^{-1}$; $k_{G,7} = 0.60\ Units$; $k_{h,7} = 0.05\ Units$. **(D)** nullcline for row **D**, table 2, parameter values: $K_{-2}/k_2 = 1.00\ Units$; $k_{e,7} = 0.70\ Units \cdot s^{-1}$; $k_{g,7} = 3.00\ Units$. $k_{f,7} = 3.50\ Units$; $k_{E,7} = 0.40\ Units \cdot s^{-1}$; $k_{G,7} = 2.70\ Units$. $k_{F,7} = 1.50\ Units$; $k_{h,7} = 0.10\ Units$. **(E)** nullcline for row **E**, table 2, parameter values: $k_{e,7} = 0.26\ Units \cdot s^{-1}$; $k_{g,7} = 1.40\ Units$. $k_{f,7} = 3.50\ Units$; $k_{h,7} = 1.30\ s^{-1}$. **(F)** nullcline for row **F**, table 2, parameter values: $K_{-2}/k_2 = 1.00\ Units$; $k_{e,7} = 0.03\ s^{-1}$; $k_{E,7} = 0.24\ s^{-1}$; $k_{G,7} = 0.15\ Units$; $k_{h,7} = 0.08\ Units$. **(G)** nullcline for row **G**, table 2, parameter values: $K_{-2}/k_2 = 1.00\ Units$; $k_{e,7} = 0.70\ s^{-1}$; $k_{E,7} = 0.02\ Units \cdot s^{-1}$; $k_{G,7} = 1.50\ Units$; $k_{F,7} = 3.50\ Units$; $k_{h,7} = 0.20\ Units$. **(H)** nullcline for row **H**, table 2, parameter values: $k_{e,7} = 0.90\ s^{-1}$; $k_{g,7} = 3.50\ Units$. $k_{E,7} = 0.50\ Units \cdot s^{-1}$; $k_{G,7} = 1.50\ Units$. $k_{F,7} = 4.50\ Units$; $k_{h,7} = 0.10\ s^{-1}$; $k_{H,7} = 0.30\ s^{-1}$; $k_{y,5} = 0.30\ Units$. **(I)** nullcline for row **I**, table 2, parameter values: $k_{e,7} = 0.20\ s^{-1}$; $k_{g,7} = 1.50\ Units$; $k_{E,7} = 0.12\ s^{-1}$; $k_{G,7} = 4.10\ Units$; $k_{h,7} = 0.04\ s^{-1}$; $k_{H,7} = 0.20\ Units \cdot s^{-1}$; $k_{y,5} = 1.20\ Units$. *Units* stands for *particle number per surface area.*

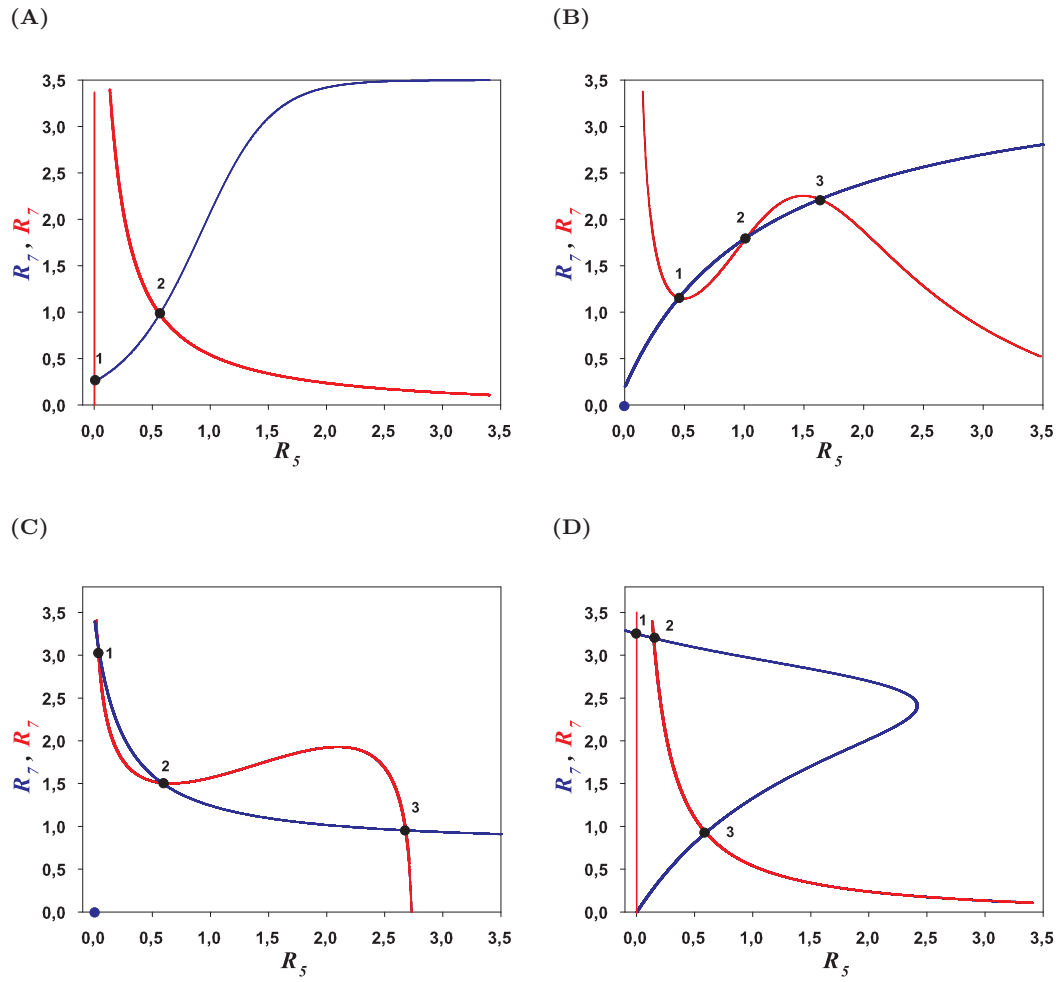

Figure 4: **Phase plane analysis of intersections of nullclines.** Parameter values are identical to those in **figures 1, 2**. **(A) Branching behavior**. Model of box **B,1** of table 2 has just two intersections independent of the specific choice of the parameter values. **(B) In-phase switch**. Model of box **A,3** of table 2. Depending on parameters the steady states 1 and 2 or 2 and 3 may coalesce and vanish, enclosing the hysteresis region. However, steady state 1 always has both concentrations lower than in steady state 3 which contradicts the experimental evidence on Rab5-Rab7 conversion. **(C) Toggle switch**. Model of box **I,3** of table 2. The relative location of the three intersections corresponds to the experimental observations. **(D) Cut-out switch**. Model of box **C,3** of table 2 also possesses the three intersections in the experimentally observed relative locations.

are the reason (from a phase plane point of view) for hysteresis in bistable systems [4]. Hence the employed strategy amounts to a bifurcation analysis.

The results of the bifurcation analysis are represented as bifurcation diagrams in **figure 4**. The corresponding simulations are shown in **figure 5**. These results confirm the phase plane analysis performed above with analytical and graphical methods. The analysis has selected two model classes, the toggle switch and the cut-out switch, out of a large set of combinatorially constructed models. In the main document we have compared the two selected models to a number of independent experimental observations and found the cut-out switch (**figures 3D, 4D, 5D** to be better supported by the experimental evidence.

4 Statistical analysis of single-endosome tracking data

4.1 Data collection

Out of a large pool of tracked early endosomes from 3 independent experiments, 28 intensity time courses have been extracted by the criterion of a vanishing Rab5 intensity at the end of the track. Track length varies widely. Each of the 28 extracted time courses was inspected manually and found to display qualitative behaviour of one of the two classes: (i) strong intensity fluctuations followed by a marked decay of intensity lasting 20 to 100 seconds and followed by very low intensity for the remaining time or (ii) a continuous intensity decay with low rate and duration of several 100 seconds. 23 tracks belong to class (i) and 5 to class (ii).

4.2 Identification of conversion time points and data synchronisation

For the 23 data sets of class (i) the start time of the marked decay was determined manually. No start time could be assigned to class (ii) data. The time axis of each set was shifted by the individual start time such that all putative conversion events synchronize at a unique time point which was chosen to be 0.

4.3 Intensity scaling

As the data sets were collected from 3 independent experiments, their overall intensities varied systematically. To compensate for this systematic deviation all intensities of experiment 1 were scaled by a constant factor 20822/20822=1, experiment 2 by 20822/13168 and experiment 3 by 20822/13636. The resulting data points are shown as dots in Fig. 4 of the main document and illustrate the large amplitude of intensity fluctuations. As an example, track 5 of experiment 1 is denoted by a full black curve. The presented time window is chosen such that even the shorter data sets cover its full range.

4.4 Intensity statistics

In order to test for a positive or negative intensity trend, we averaged all 23 data points at each time point which is denoted by the green curve. The gray interval indicates 70% confidence around the average (green curve). We note that the averaged intensities possess a local minimum about 50 seconds before the putative conversion start at maximum intensity. The reason is not clear and may well be pure coincidence. For the selection among the possible models it is essential to discriminate a positive from a negative slope of $R_5(t)$ before conversion. The analysed data shows a positive slope which is consistent with the predictions of the cut-out switch.

References

[1] Ferrell J. E. *2002; Curr. Opin. Cell Biol. 14 (2), 140-148*

[2] Cinquin O. *2007; PLoS Comput Biol. 16; 3(2)*

[3] Doedel E., Keller H. B., Kernevez J. P. *1991; Int. J. Bif. Chaos 1 (3), 745-772.*

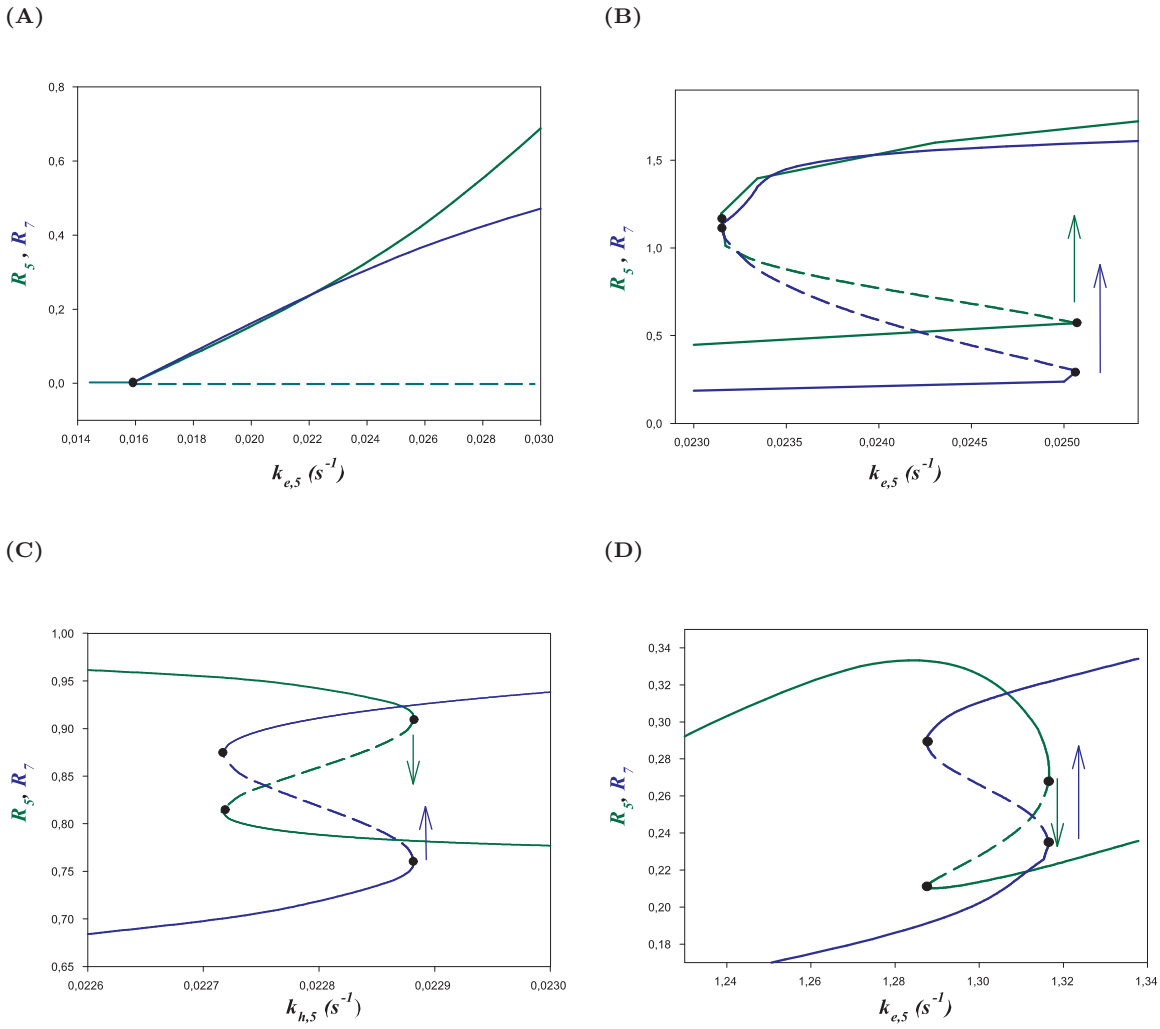

Figure 5: **Bifurcation analysis.** Bold lines indicate stable steady states, dashed unstable states. Green lines denote Rab5, blue lines denote Rab7. The limits of the bistability area are marked by black dots. Arrows denote branch switching when the control parameter is slowly increased in numerical simulations. The choice of the control parameter is arbitrary and the particular choice served demonstration purposes only. **(A) Branching behavior**. Model of box **A,2** of table 2 and figure 3A. **(B) In Phase Switch**. Model of box **B,4** of table 2 and figure 3B. **(C) Toggle Switch**. Model of box **C,5** of table 2 and figure 3C. Parameter values: $k_{e,5} = 0.06\ s^{-1}$; $k_{g,5} = 0.5\ Units$; $k_{H,5} = 0.30\ s^{-1}$; $k_{g,7} = 0.10\ Units$; $k_{G,7} = 1.060\ Units$; $k_{h,7} = 0.05\ Units$. **(D) Cut-Out Switch**. Model of box **D,6** of table 2 and figure 3D. Parameter values: $k_{i,5} = 0.06\ Units$; $k_{m,5} = 0.06\ Units$; $k_{h,5} = 0.01\ s^{-1}$. $k_{e,7} = 0.35\ s^{-1}$; $k_{E,7} = 0.03\ s^{-1}$; $k_{G,7} = 0.80\ Units$; Other values are identical to those in **figures 1,2,3**.

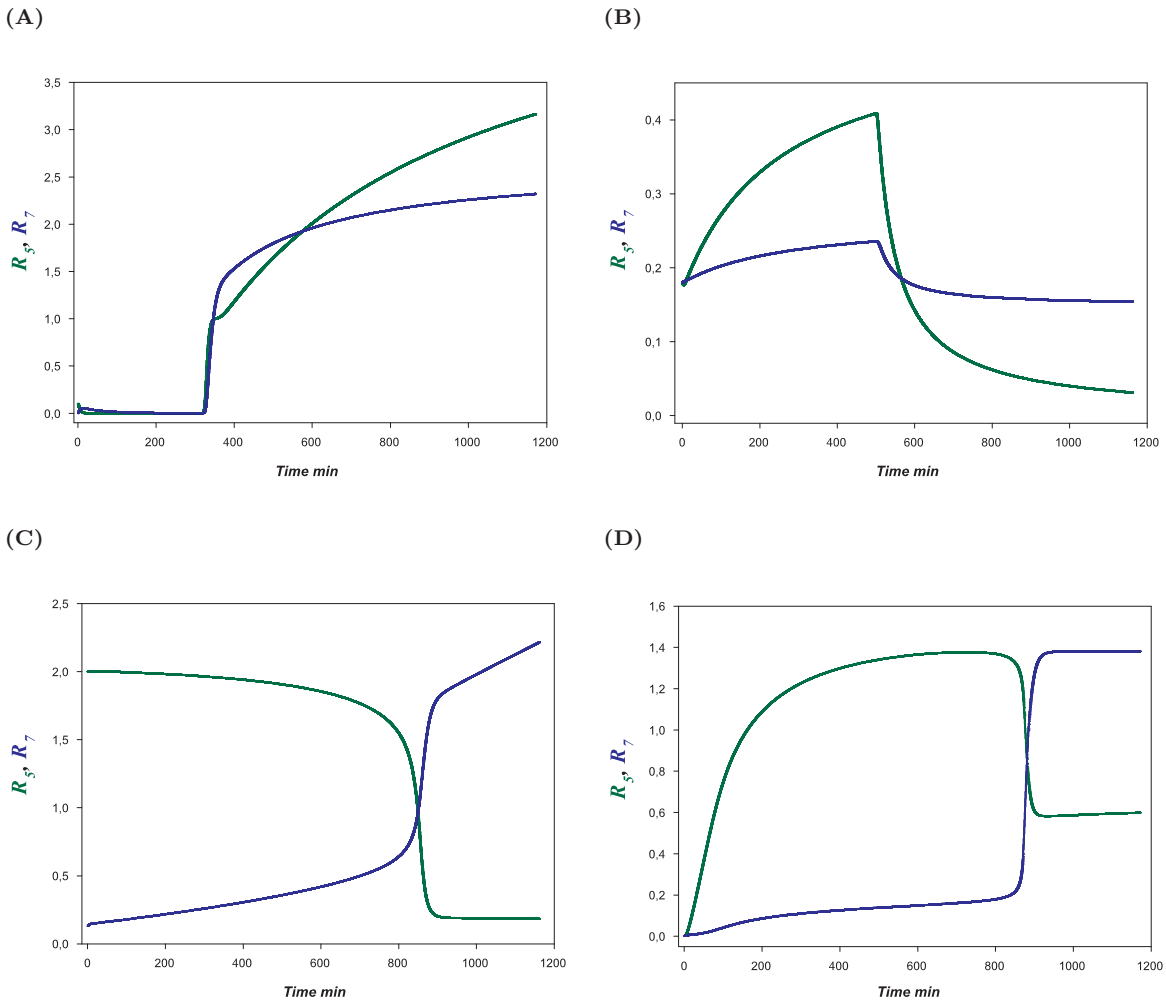

Figure 6: **Numerical simulations.** Green lines denote Rab5, blue lines denote Rab7. Parameter values are identical to those in **figures 1,2,3**. During the numerical simulations, the control parameter is slowly increased such that it spans the bistable regions in the bifurcation diagrams, (**figure 4**). **(A) Branching behavior**. Model of box **A,2** of table 2 and figures 3A, 4A. **(B) In Phase Switch**. Model of box **B,4** of table 2 and figures 3B, 4B. **(C) Toggle Switch**. Model of box **C,5** of table 2 and figures 3C, 4C. **(D) Cut-Out Switch**. Model of box **D,6** of table 2 and figures 3D, 4D. Parameter values are identical to those in **figures 5**.

[4] Tyson J. J., Chen K. C. and Novak B. *2003; Curr. Opin. Cell Biol. 15, 221-231*